A Preliminary Assessment of Pareto Optimization for a Gas-Lift Enhanced PMFR Primary System under Fuel Inventory Constraints

Jihun Im[a], JinHo Song[a], Joon-Eon Yang[a], Sung Joong Kim[a, b*]
[a] *Department of Nuclear Engineering, Hanyang University, 222 Wangsimni-ro, Seongdong-gu,Seoul 04763, Republic of Korea*
[b] *Institute of Nano Science and Technology, Hanyang University, 222 Wangsimni-ro, Seongdong-gu, Seoul 04763, Republic of Korea*

***Keywords :** Molten salt reactor; Passive molten salt reactor; SCO_2 Power cycle; Electrolysis; Hydrogen Production

1. Introduction

To achieve net-zero emissions and mitigate climate change [1-3], Molten Salt Reactors (MSRs) have emerged as a promising carbon-free alternative [4, 5, 10]. Driven by the need for inherent safety, proliferation resistance, and high-temperature heat supply, the I-SAFE-MSR initiative is developing the Passive Molten Salt Fast Reactor (PMFR) [7, 8, 11]. Designed with a fast-spectrum core utilizing highly costly High-Assay Low-Enriched Uranium(HALEU), the PMFR targets over 30 years of continuous operation without refueling.

While the PMFR prioritizes inherent safety through natural circulation cooling [8, 11], scaling the system to a 300 MWt demonstration level introduces severe thermal-hydraulic challenges. Because the molten salt serves as both coolant and fuel, the physical volume of the primary loop must be strictly minimized to limit the out-of-core HALEU inventory [4, 18]. This necessitates a highly compact heat exchanger, which can lead to a sharp increase in primary-side flow resistance, making it highly challenging for the natural circulation driving force alone to balance the system [8, 9, 16, 17].

In neutronic core design, calculating the burnup based on a fixed core geometry and thermal power determines the exact total fuel inventory required to achieve the targeted 30-year operational cycle. By strictly confining the out-of-core primary loop volume to this predefined fuel inventory limit, the system secures significant economic and safety benefits by avoiding the addition of highly costly nuclear fuel solely to enhance the natural circulation driving force. To achieve this, this study proposes a comprehensive multi-variable optimization approach from a system design perspective. To overcome the increased friction without expanding the loop size beyond the inventory limit, a gas-lift system, injecting inert helium gas at the bottom of the riser to provide additional buoyancy, is introduced [7, 9]. Within this context, the overarching system geometry and heat exchanger parameters were parameterized to systematically evaluate the complex trade-offs among the natural circulation driving force, frictional pressure drop, and Logarithmic Mean Temperature Difference (LMTD). Ultimately, this optimization identifies the optimal design space that maximizes thermal-hydraulic performance while strictly satisfying the critical fuel inventory constraints of the PMFR.

2. 1D Thermal-Hydraulic Model

To evaluate the natural circulation driving force and heat transfer performance, an in-house 1D coupled thermal-hydraulic code was developed [7, 8]. The primary system consists of the reactor core, a vertical riser for helium gas-lift, and a shell-and-tube helical coil heat exchanger [11]. The heat transfer and pressure drop within the helical tube geometry are rigorously evaluated using established correlations for curved pipes and crossflow [19-21]. Concurrently, the Drift-Flux model is utilized to calculate the local void fraction of the helium-molten salt two-phase flow in the vertical riser [7, 22].

A distinctive feature of this hydraulic model is the mechanistic derivation of the two-phase pressure drop, rather than relying solely on conventional empirical two-phase friction multiplier correlations [15]. Because the injected helium gas occupies a fraction of the flow area, the actual velocity of the liquid phase in the narrowed channel is physically defined using the superficial liquid velocity and the local void fraction [22]:

$$u_L = \frac{j_L}{1-\alpha}$$

Assuming a turbulent flow regime where the friction factor follows the Blasius-type dependency ($f \propto u_L^{-0.2}$), the two-phase frictional pressure drop (ΔP_{TP}), which is proportional to $f \cdot u_L^2$, can be expressed as:

$$\Delta P_{TP} \propto u_L^{1.8} = \left(\frac{j_L}{1-\alpha}\right)^{1.8}$$

This fundamental mechanistic approach naturally yields a two-phase friction multiplier of $\phi_f^2 = (1-\alpha)^{-1.8}$, which simplifies to:

$$\phi_f = (1-\alpha)^{-0.9}$$

As illustrated in Fig. 1, extensive experimental data for vertical two-phase flow demonstrate excellent agreement with the ϕ_f −correlation where the exponent

n is closely bounded between 0.875 and 0.9 [23]. By directly computing the local actual liquid velocity through the area reduction factor $(1-\alpha)$ and applying the fundamental friction factor f, the implemented code naturally reproduces this empirical n=0.9 behavior. This confirms that the code's direct mechanistic calculation intrinsically captures the complex two-phase friction phenomena, fully justifying the accuracy of the hydraulic model without requiring artificial empirical tuning.

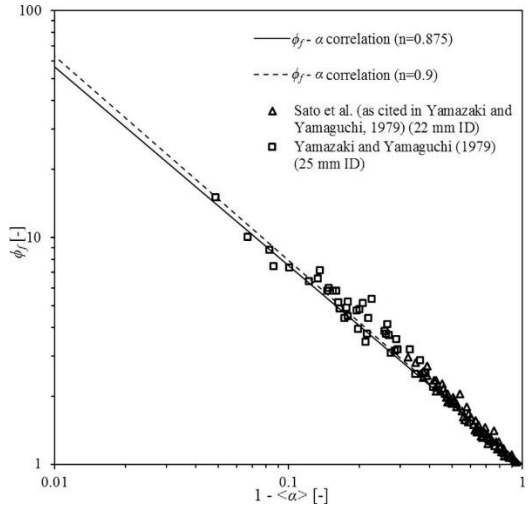

Figure 1. Comparison of the two-phase friction multiplier $(\boldsymbol{\phi_f})$ as a function of the liquid fraction $(\mathbf{1}-\langle\boldsymbol{\alpha}\rangle)$ [23].

The thermal-hydraulic performance of the Helical Coil Heat Exchanger (HCHX) is evaluated using empirical correlations: Schmidt and Mori-Nakayama for the tube-side [20, 21], and Žukauskas for shell-side crossflow [19]. The coil's ascent angle dictates critical system trade-offs. On the shell-side, a smaller angle of attack (90° minus the ascent angle) inherently reduces both pressure loss and the heat transfer coefficient [19]. Simultaneously, on the tube-side, the ascent angle constrains the bundle geometry; smaller angles yield longer but fewer tubes per helix, while larger angles accommodate more, albeit shorter, tubes.

To ensure reliability, the 1D MATLAB model was rigorously verified against 3D CFD simulations. As illustrated in Fig. 2, the parity plots demonstrate excellent agreement for shell-side Nusselt (Nu) and Euler (Eu) numbers, as well as tube-side heat transfer rates and pressure drops. This successful verification confirms the 1D model as an accurate and computationally efficient foundation for the comprehensive multi-variable optimization.

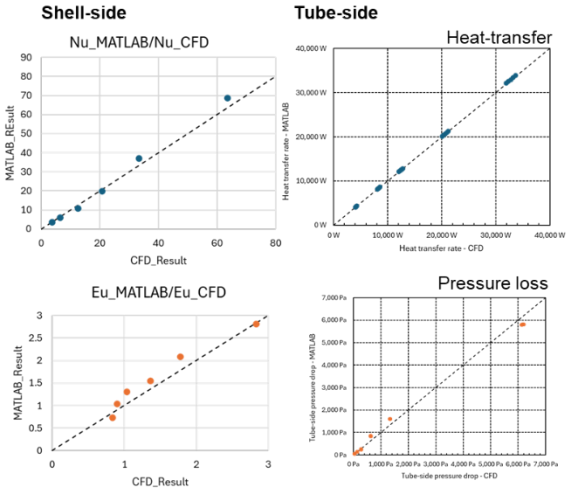

Figure 2. Verification of the 1D MATLAB HCHX model against 3D CFD simulations.

3. Design Space and Pareto Optimization Framework

To systematically evaluate the 300 MWt PMFR thermal-hydraulic trade-offs, a discrete multi-variable design space was established, encompassing the gas-lift riser (height, radius) and HCHX geometry (tube diameter, ascent angle). To strictly conserve the out-of-core fuel inventory, an optimization subroutine dynamically determines the HCHX active length and radial tube layers for each configuration. For consistent performance evaluation, the secondary-side mass flow rate is fixed, while its temperature is iteratively adjusted to maintain a constant primary-side outlet temperature. The specific variable ranges are summarized in the subsequent table.

Table. 1. Geometric design variables and discrete search space for multi-variable optimization.

Design Variable	Range / Discrete Values
Riser Height	2 – 11 m (1 m increment)
Riser Radius	0.3, 0.4, 0.5 m
Tube outer diameter	12, 15, 18 mm
Maximum ascent angle	30°, 45°, 60°
Number of radial tube layers	Dynamically determined
Active tube length	Dynamically determined

A three-phase optimization framework was then executed to balance heat exchanger compactness and required buoyancy. Phase 1 performs a global search using the 1D model to calculate the LMTD and the required pressure ratio (total friction over natural circulation head) for all valid configurations. Phase 2 extracts the Pareto frontier by minimizing both the LMTD and the required pressure ratio. Finally, Phase 3 applies a bisection algorithm along the Pareto frontier to pinpoint optimal designs that strictly satisfy discrete maximum void fraction limits (5%, 10%, 15%, 20%, and 25%).

4. Results and Discussion

The multi-variable optimization results for the 300 MWt PMFR primary system are presented in Fig. 3. The extracted Pareto frontier (solid red line) illustrates the trade-off between the LMTD and the Pressure Ratio (total friction over single phase natural circulation head). To achieve a pure natural circulation regime (Pressure Ratio < 1), the HCHX geometry must be designed to minimize frictional resistance, which typically involves lower flow velocities and wider channel spacings. This hydraulic relaxation can significantly degrade heat transfer coefficient, requiring a high LMTD (exceeding 150°C) to transfer the target 300 MWt within the restricted volume. Such a large temperature difference would likely impose a severe penalty on the secondary-side power conversion efficiency.

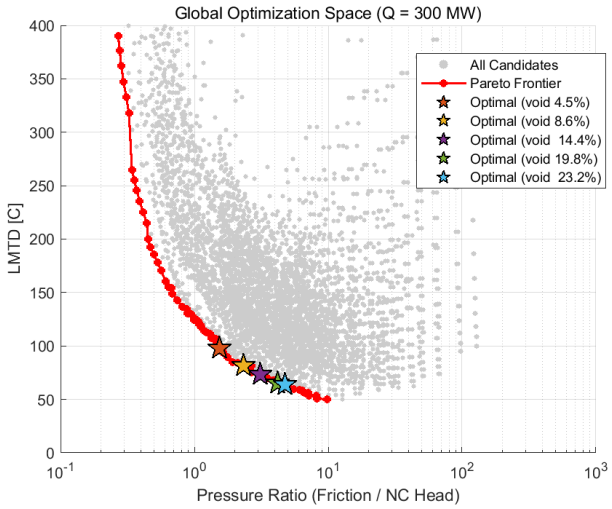

Figure 3 Global Pareto optimization space for the 300 MWt PMFR. The Pareto frontier highlights the trade-off between LMTD and the required Pressure Ratio

The helium gas-lift offers a viable pathway to overcome this thermal-hydraulic bottleneck. The star markers in Fig. 3 represent optimal configurations that satisfy specific void fraction limits (ranging from 4.5% to 23.2%). As the allowable void fraction increases, the enhanced buoyancy accommodates a higher-pressure ratio (shifting from approximately 1.5 to 7). This allows for the adoption of HCHX geometries with a higher fluid velocities, which in turn elevates and reduces the required LMTD from approximately 100°C (at a 4.5% void limit) to roughly 65°C (at a 23.2% limit).

However, a clear trend of diminishing returns is observed as the void fraction increases beyond approximately 15%. This phenomenon can be physically attributed to the non-linear nature of the two-phase friction multiplier established in the methodology. At lower void fractions, the increase in gas-lift buoyancy dominates, supplying a substantial net driving force that drastically reduces the LMTD. Conversely, as the void fraction exceeds 15%, the frictional penalty driven by the two-phase multiplier accelerates. This rapidly growing two-phase flow resistance begins to cancel out the additional buoyancy, yielding only marginal net improvements in the thermal-hydraulic performance. Consequently, this suggests the existence of an optimal design window, approximately between 10% and 15% void fraction, where the heat transfer performance is maximized before the two-phase frictional penalty becomes prohibitive, all while avoiding excessive flow instability penalties to the core.

5. Conclusion

This study proposed a comprehensive multi-variable optimization framework for the primary heat transport system of a 300 MWt PMFR, strictly constrained by the out-of-core fuel inventory limit. By developing a 1D thermal-hydraulic model featuring a mechanistically derived two-phase friction multiplier and executing a three-phase Pareto optimization, the fundamental trade-offs between heat exchanger performance and gas-lift motive force were quantitatively evaluated. The results demonstrated that implementing a helium gas-lift system substantially enhances the overall heat transfer performance by enabling the adoption of a larger heat exchanger at the expense of increased pressure drop within the restricted loop volume, allowing for a drastic reduction in the required LMTD. However, as the void fraction exceeds approximately 15%, the non-linearly accelerating two-phase frictional penalty begins to negate the additional buoyancy, resulting in marginal thermal improvements. This physical phenomenon dictates an optimal design window, between 10% and 15% void fraction, where thermal-hydraulic performance is maximized without inducing excessive flow instability or potential penalties to the core.

Acknowledgements

This research was supported by the National Research Foundation of Korea (NRF) and funded by the ministry of Science, ICT, and Future Planning, Republic of Korea (grant numbers NRF-2021M2D2A2076382) and supported by the Human Resources Development of the Korea Institute of Energy Technology Evaluation and Planning (KETEP) grant funded by the Korea

government Ministry of Knowledge Economy (RS-2024-00439210).

REFERENCES

[1] IPCC, "Summary for Policymakers," in Climate Change 2022: Impacts, Adaptation, and Vulnerability, Contribution of Working Group II to the Sixth Assessment Report of the Intergovernmental Panel on Climate Change, Cambridge University Press, Cambridge, UK and New York, NY, USA (2022).

[2] IPCC, Climate Change 2022: Impacts, Adaptation, and Vulnerability, Contribution of Working Group II to the Sixth Assessment Report of the Intergovernmental Panel on Climate Change, Cambridge University Press, Cambridge, UK and New York, NY, USA (2022).

[3] IEA, World Energy Outlook 2022, IEA, Paris (2022).

[4] J. Serp, M. Allibert, O. Beneš, S. Delpech, O. Feynberg, V. Ghetta, D. Heuer, D. Holcomb, V. Ignatiev, J.L. Kloosterman, L. Luzzi, E. Merle-Lucotte, J. Uhlíř, R. Yoshioka, and D. Zhimin, "The molten salt reactor (MSR) in Generation IV: Overview and perspectives," Prog. Nucl. Energy 77, pp. 308–319 (2014).

[5] T.J. Dolan, Molten Salt Reactors and Thorium Energy, Woodhead Publishing, Cambridge, USA (2017).

[6] R. Sharma, A. Delebarre, and B. Allappat, "Chemical-looping combustion – an overview and application of the recirculating fluidized bed reactor for improvement," Int. J. Energy Res. 36, pp. 1331–1350 (2014). https://doi.org/10.1002/er.3151.

[7] Choi, W.J., et al., 2024. Experimental and numerical assessment of helium bubble lift during natural circulation for passive molten salt fast reactor. Nuclear Engineering and Technology 56(3), 1002–1012. https://doi.org/10.1016/j.net.2023.12.016.

[8] Lee, Juhyeong, et al., 2025. Multiphysics Analysis of Natural Circulation-Driven Operation of Passive Molten Salt Fast Reactor and Effect of Guide Structure. International Journal of Energy Research 2025(1), 6052359.

[9] Lim, J., et al., 2021. Preliminary analysis of the effect of the gas injection on natural circulation for molten salt reactor type small modular reactor system operated without a pump. Transactions of the Korean Nuclear Society Virtual Autumn Meeting, October 21–22.

[10] Kim, H., Kwon, C., Ham, S., Lee, J., Kim, S.J., Kim, S., 2023. Physical properties of KCl-UCl3 molten salts as potential fuels for molten salt reactors. Journal of Nuclear Materials 577, 154329. https://doi.org/10.1016/j.jnucmat.2023.154329.

[11] Park, J.H., et al., 2022. Design concepts and requirements of passive molten salt fast reactor (PMFR). Transactions of the Korean Nuclear Society Spring Meeting.

[12] J. Fuger, V.B. Parker, W.N. Hubbard, and F.L. Oetting, The Chemical Thermodynamics of Actinide Elements and Compounds: Pt 8. The Actinide Halides, International Atomic Energy Agency, Vienna (1983).

[13] S. Katyshev, Yu Chervinskii, and V. Desyatnik, "Density and viscosity of fused mixtures of uranium chlorides and potassium chloride," At. Energy (1982).

[14] M.W. Chase Jr., NIST-JANAF Thermochemical Tables, Fourth Edition, J. Phys. Chem. Ref. Data, Monograph 9 (1998).

[15] R.W. Lockhart and R.W. Martinelli, "Proposed correlation of data for isothermal two-phase, two-component flow in pipes," Chem. Eng. Process. 45, pp. 39–48 (1949).

[16] D.T. Ingersoll et al., "NuScale small modular reactor for co-generation of electricity and water," Desalination 340, pp. 84–93 (2014).

[17] P. Sabharwall et al., Process Heat Exchanger Options for Fluoride Salt High Temperature Reactor, INL/EXT-11-21584, Idaho National Lab. (INL), Idaho Falls, ID, USA (2011).

[18] Robertson, R. C. (1971). CONCEPTUAL DESIGN STUDY OF A SINGLE-FLUID MOLTEN-SALT BREEDER REACTOR (No. ORNL-4541). comp.; Oak Ridge National Lab.(ORNL), Oak Ridge, TN (United States).

[19] Zukauskas and R. Ulinskas, Heat Transfer in Tube Banks in Crossflow (1988).

[20] Y. Mori and W. Nakayama, "Study on forced convective heat transfer in curved pipes: (3rd report, theoretical analysis under the condition of uniform wall temperature and practical formulae)," Int. J. Heat Mass Transfer 10(5), pp. 681-695 (1967).

[21] E.F. Schmidt, "Wärmeübergang und druckverlust in rohrschlangen," Chem. Ing. Tech. 39(13) (1967).

[22] White, Frank M. "Fluid mechanics." (2011).

[23] Lu, C., Kong, R., Qiao, S., Larimer, J., Kim, S., Bajorek, S., ... & Hoxie, C. (2018). Frictional pressure drop analysis for horizontal and vertical air-water two-phase flows in different pipe sizes. *Nuclear Engineering and Design*, *332*, 147-161.